

ground. With the updoming of Tharsis, the resulting gradient in hydraulic head may have driven the flow of groundwater to lower elevations where the local increase in hydraulic pressure was sufficient to disrupt the confining layer and permit the catastrophic discharge of groundwater to the surface [6]. With the continued growth of Tharsis, the development of destabilizing hydraulic pressures should have occurred at progressively greater distances from the central uplift, resulting in potentially testable correlations between channel elevation [which varies from a high of 7 km for Kasei Vallis ($0^{\circ}, 80^{\circ}$) to a low of 0 km for Ares Vallis ($-2^{\circ}, 18^{\circ}$)], distance, and age. Alternatively, the growth of tensional fractures associated with the updoming of Tharsis and rifting of Valles Marineris may have broken the confining layer of frozen ground and permitted the discharge of groundwater to the surface as the fractures propagated to the lower elevations toward the east [8]. Recent calculations also suggest that channel activity may have been seismically triggered [9,10]. By this mechanism, shock waves generated by impacts, earthquakes, or explosive volcanic eruptions may have generated transient pore pressures sufficient to disrupt the confining layer of ground ice, permitting groundwater to flow onto the surface driven by whatever artesian pressure existed within the confined aquifer prior to the seismic event. It should be noted that these scenarios are not mutually exclusive, nor do they exhaust the number of possible mechanisms for generating the Chryse or other Late Hesperian channels.

Unlike the majority of channels that were active during the Late Hesperian, many Early and Middle Amazonian channels appear related (both spatially and temporally) to regions of likely geothermal activity. For example, in the region east of Hellas, Dao, Reull, and Harmahkis Valles are all located within several hundred kilometers of the Early Hesperian volcano Hadriaca Patera ($-31^{\circ}, 268^{\circ}$) and appear closely associated with lava flows from the Late Hesperian-Early Amazonian volcano Tyrhena Patera ($-22^{\circ}, 254^{\circ}$) [11]. Another major concentration of channels occurs to the west and northwest of Elysium Mons ($25^{\circ}, 213^{\circ}$) and Hecates Tholus ($32^{\circ}, 210^{\circ}$), volcanos that were also thought to have been active during this period. Both the geologic setting and chronology of these channels suggests that they may have been fed by water melted as a result of the increased heat flow associated with local volcanism. The accumulated water may then have been released to the surface either by the eventual thawing of the ground-ice layer or by its mechanical disruption through the build-up of a large hydraulic head. The average elevation of channel source regions during this period is ~ 1 km, or approximately 2 km lower than the apparent average elevation of Late Hesperian channels.

A number of small Middle- to Late-Amazonian-aged channels have been identified to the east and southeast of the Olympus Mons escarpment [12], a relationship that again suggests a potential geothermal origin. There is also evidence of fluvial activity within Ophir Chasma ($-4^{\circ}, 73^{\circ}$), which may be water-rich debris flows [13,14]. The most significant outflow event to have occurred during this time happened near Cerberus Rupes ($8^{\circ}, 195^{\circ}$), where a large broad swath of predominantly featureless, sparsely cratered terrain lies within a topographic basin that covers an area of $\sim 10^6$ km² to the south of the fracture. With the exception of a few moderately sized areas located in the eastern half of the basin, the morphologic evidence is more consistent with a major ponding feature, such as a lake or sea, than with the type of outflow channel found in the Chryse system. The ultimate source of water that embayed this

region was apparently a subsurface reservoir that was either breached by the formation of Cerberus Rupes or which, at some later time, was able to take advantage of the structural pathway provided by the existence of the fracture to reach the surface [15].

Summary: Outflow channel activity has apparently spanned most of martian geologic history, from the Late Noachian to Late Amazonian. The outflow channels that date back to the Late Noachian and Early Hesperian are few in number and exhibit no strong association with any single geographic region. The Late Hesperian saw a widespread and significant increase in channel activity, much of which was concentrated in the Chryse system, a distribution that is probably linked to the concurrent development of Tharsis and Valles Marineris. During the Amazonian, the occurrence of outflow channels appears to have become more localized around regions of potential geothermal activity. One possible explanation for this geographic shift in outflow channel activity is that by the Early Amazonian the cryosphere had grown thick enough that it was no longer easily susceptible to disruption by artesian pressure alone. Alternatively, the cryosphere may have simply grown so large that no groundwater, outside that transiently produced by the melting of ground ice in active geothermal regions, survived beyond the Late Hesperian. If this last interpretation is true, theoretical calculations indicate that the amount of H₂O required to saturate the pore volume of the cryosphere at this time would still exceed the equivalent of a global ocean many hundreds of meters deep [16]. A more detailed analysis of these results is currently in preparation.

References: [1] Tanaka K. L. (1986) *Proc. LPS 16th*, in *JGR*, 91, E139-E158. [2] U.S.G.S. (1991) *Map 1-2160*. [3] Greeley R. and Guest J. E. (1987) *U.S.G.S. Map 1-1802-B*. [4] Rotto S. L. and Tanaka K. L. (1990) *LPS XXIII*, 1173-1174. [5] Scott D. H. and Tanaka K. L. (1987) *U.S.G.S. Map 1-1802-A*. [6] Carr M. H. (1979) *JGR*, 84, 2995-3007. [7] Coates D. R. (1983) in *Mega-Geomorphology*, Oxford, 240. [8] Masursky et al. (1977) *JGR*, 82, 4016-4038. [9] Leyva I. A. and Clifford S. M. (1993) *LPS XXIV*, 875-876. [10] Tanaka K. L. and Clifford S. M. (1993) *LPI Tech. Rpt. 93-04*, 17-18. [11] Crown D. A. et al. (1992) *Icarus*, 100, 1-25. [12] Mouginis-Mark P. J. (1990) *Icarus*, 84, 362-373. [13] Witbeck N. E. et al. (1991) *U.S.G.S. Map 1-2010*. [14] Lucchitta B. K. (1987) *Icarus*, 72, 411-429. [15] Tanaka K. L. and Scott D. H. (1986) *LPS XVII*, 865-866. [16] Clifford S. M. (1993) *JGR*, 98, 10973-11016.

N94-33236

546 91 185.0267

OBLIQUITY VARIATION IN A MARS CLIMATE EVOLUTION MODEL. D. Tyler^{1,2} and R. M. Haberle², ¹Department of Meteorology, San Jose State University, San Jose CA 95192, USA, ²Ames Research Center, Moffett Field CA 94035-1000, USA.

The existence of layered terrain in both polar regions of Mars is strong evidence supporting a cyclic variation in climate. It has been suggested [1] that periods of net deposition have alternated with periods of net erosion in creating the layered structure that is seen today. The cause for this cyclic climatic behavior is variation in the annually averaged latitudinal distribution of solar insolation in response to obliquity cycles [2]. For Mars, obliquity variation leads to major climatological excursions due to the condensation and sublimation of the major atmospheric constituent, CO₂. The atmosphere will collapse into polar caps, or existing caps will rapidly sublimate into the atmosphere, dependent upon the polar surface

As has been shown in terrestrial snow, experimentally [1] and theoretically [2], the dielectric constant is not just a very good indicator of the density of snow, but also gives information on the texture of the particles. The ratio between water- and CO_2 -ice can be determined. On the other hand, on soil or rocky ground the porosity and, to some extent, the composition of the material can be investigated. Since the landers are supposed to operate for an extended period of time, diurnal and annual changes in the ground (e.g., by CO_2 or water frost) can be studied. The discussed quadrupole experiment will also measure into some depth (usually in the range of the dimension of the quadrupole) and detect buried boulders or cavities.

One instrument uses very small high-frequency antennas, similar to the ones used during the KOSI (comet simulation) experiments, performed in the large space simulator in Cologne, Germany [3]. These antennas would have a resonance frequency somewhere between 1 and 12 GHz. So far, $\lambda/4$ groundplane structures have been tested, but other arrangements, e.g., $\lambda/2$ dipole-antennas, could be used as well. The traditional microwave bridge method could be used, but instead of using a waveguide containing the sample material, the antennas should be used as sensors. These sensors (with dimensions of a few centimeters) have to be in contact with the ground as shown in Fig. 1. By determining the actual resonance frequency ν_{res} (which is a function of the dimension of the sensor and the dielectric constant of the surrounding medium), the surface material is analyzed.

The advantage of this kind of instrument is its extreme low weight and low power demand. The sensor could be placed underneath the lander, e.g., on the bottom side of a landing leg. The electronics consist mainly of a sweep oscillator and a simplified swept amplitude analyzer, which finds ν_{res} of the antennas. Using a groundplane antenna, there is little or no influence by the lander body on the measurement. On the other hand, the antenna has to be embedded in the ground material. This is no major problem in case of soil or snow-ice, but problematic in case of rocks, since the sensor has to be embedded in material of a grain size, small compared to its own dimensions.

The second instrument is based on a principle that was first discussed by Wenner in 1915 [4] and Schlumberger 1920 [5]. The method was used originally to make Earth-resistivity maps of special areas and is nowadays basically used as a tool in archeology. Four electrodes form a quasistatic (the commonly used frequency is around 15 kHz) quadrupole. When an alternating current I is injected into two of the electrodes, a voltage V is induced between the other two. Thus, one obtains the mutual impedance of the quadrupole

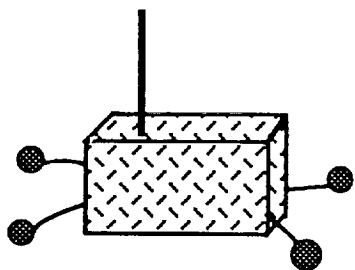


Fig. 2. Arrangement of quasistatic quadrupole.

pole ($Z = V/I$), which is a function of ϵ of the ground. Traditionally, the four electrodes are stuck into the ground, but it has been shown that the measurement is also possible if the electrodes are just above the surface [6,7]. Also, the traditional linear configuration can be modified into a square configuration [6], as shown in Fig. 2.

References: [1] Tiuri M. et al. (1984) *IEEE J. of Oceanic Eng.*, Vol. OE-9 (5). [2] Priou A. (1992) *Dielectric Properties of Heterogeneous Materials*, Elsevier. [3] Ulamec S. et al. (1993) *LPS XXIV*, 1451–1452. [4] Wenner F. (1915) *Bull., 12 Sci. Paper* 259, U.S. Bureau of Standards, 469–478. [5] Schlumberger C. (1920) *Etude de la Prospection Electrique du Sous-Sol*, Gauthier-Villars, Paris. [6] Grard R. (1991) *Meas. Sci. Technol.*, 1, 295–301. [7] Grard R. and Tabbagh A. (1991) *JGR*, 96, 4117–4123.

N94-33237

54891 NBS. 01

THE INFLUENCE OF THERMAL INERTIA ON MARS' SEASONAL PRESSURE VARIATION AND THE EFFECT OF THE "WEATHER" COMPONENT. S. E. Wood and D. A. Paige, University of California, Los Angeles CA 90024, USA.

Using a Leighton-Murray type [1] diurnal and seasonal Mars thermal model, we found that it is possible to reproduce the seasonal variation in daily-average pressures (~680–890 Pa) measured by Viking Lander 1 (VL1), during years without global dust storms, with a standard deviation of less than 5 Pa [2]. In this simple model, surface CO_2 frost condensation and sublimation rates at each latitude are determined by the net effects of radiation, latent heat, and heat conduction in subsurface soil layers. An inherent assumption of our model is that the seasonal pressure variation is due entirely to the exchange of mass between the atmosphere and polar caps. However, the results of recent Mars GCM modeling [3,4] have made it clear that there is a significant dynamical contribution to the seasonal pressure variation. This "weather" component is primarily due to large-scale changes in atmospheric circulation, and its magnitude depends somewhat on the dust content of the atmosphere. The overall form of the theoretical weather component at the location of VL1, as calculated by the AMES GCM [3], remains the same over the typical range of Mars dust opacities (Fig. 1c). Assuming that $\tau = 0.3$ is representative of years without global dust storms, we subtracted the corresponding theoretical weather component at VL1 from the years 2 and 3 data to obtain the seasonal pressure variation due only to changes in the mass of the atmosphere. We found that fitting this new pressure curve allowed us to also fit the observed seasonal polar cap boundaries during their growth [5] and retreat [6,7] much better than before, and for more "reasonable" values of thermal inertia, frost albedo, and frost emissivity. However, the significance of this result depends on the ability of Mars GCMs to calculate the actual dynamical component at VL1, which is in turn limited by uncertainties in the available data on dust opacities. Furthermore, despite the importance of the weather component, it will be shown that the "thermal inertia component" could also be responsible for a large part of the seasonal pressure variations at VL1 given our current lack of knowledge regarding thermal inertias on Mars below diurnal skin depths.

As all studies of the seasonal CO_2 cycle [1–3,8] have demonstrated, the radiative properties of the CO_2 frost on Mars are key parameters, and obtaining good measurements of their actual values would be extremely beneficial to our ability to model and under-